JOURNAL OF MATERIALS SCIENCE **38** (2003) 575–580

Effect of tempering temperature and frequency on fatigue crack propagation in 0.2% carbon alloy steel

A. AMIRAT, K. CHAOUI
Laboratoire de Recherche Mécanique des Matériaux et Maintenance Industrielle (LR3MI), Département de Génie Mécanique, Faculté des Sciences de l'Ingénieur, Université Badji Mokhtar, BP 12, Annaba 23000, Algeria
E-mail: amirat_abd@yahoo.fr; chaoui_k@yahoo.fr

Fatigue crack growth (FCG) has been investigated in air, under high and low frequencies for lower and upper tempering temperatures, on a mining chain steel. The effect of frequency over the range tested is revealed to be not negligible in the near threshold region of ΔK_I. For growth rates greater than 10^{-5} mm/cycle, FCG rates for tests conducted at 0.6 Hz were up to 1.5 higher than FCG rates for tests conducted at 78 Hz. Tempering at 500°C produced slightly lower early stage growth rates than tempering at 200°C where the remaining residual stresses still contribute in affecting the near threshold region, for the two test frequencies. Otherwise at higher values of ΔK_I, the FCG curves were coincident. Using an empirical relationship between the constants of the Paris-Erdogan law, a correlation is established for this steel taking into account both effects of frequency and tempering. The obtained results are compared to analyzed data from literature for a high tensile steel and a linear relationship between the parameters C and n is deduced for both materials.

1. Introduction

Fatigue of metals remains an important cause of structure failures despite the considerable engineering and scientific efforts which have been devoted to the characterization of the fatigue response and to the understanding of the mechanisms of crack propagation involved [1–4]. The need for such characterization and understanding is essential to structure as design, service life prediction, development and assessment of fatigue resistant alloys [5–9]. Mining chains are examples of structures, which might contain microscopic defects and stress concentrators that may lead to failure. High strength low alloy steels in the quenched and tempered conditions are currently used for their manufacture because of the acceptable resistance to external loadings. Low tempering temperatures are chosen in order to maintain high strength levels and good wear resistance. This choice is related to residual stress magnitude, which should be systematically controlled due to the demand for a greater reliability of these structural components [10, 11]. However, residual stresses generated after quenching may not be annealed out at low tempering temperature and this led to a large number of questions on their effects on fatigue crack growth [12–15]. Investigation of the effect of microstructure in a typical mining chain W1.6753 steel [16], for low stress ratios revealed that tempering at 500°C resulted in lower near threshold fatigue crack growth rate than tempering at lower temperatures. The crack front was also delayed in the center of the tested specimen. This result was attributed to the relief of the residual stresses causing crack closure at low stress ratios. Similar effects and observations were reported when studying the heat treatment pre-strain and residual stresses [17] in a C-Mn-B mining steel. In this case, compressive residual stresses appeared to be a direct consequence of the crack retardation in the center of the specimen. Nevertheless, this retardation not only depends on the residual stress field but specifically at near threshold fatigue crack growth the crack surface roughness largely determines ΔK_{th} [3, 4, 18, 19].

Earlier before, an IRSID report largely investigated the effects of tempering temperatures on fatigue crack growth in various steel grades [20]. Generally, the main observation was that the lower the tempering temperature the faster the fatigue crack growth rate. The S-shaped curves obtained were limited to stage II and some important parameters regarding unstable region and the near threshold region were not reported. Nevertheless, the results remain a good reference for comparison. Many workers [20–23] demonstrated the susceptibility of fatigue crack growth to frequency in air and other environments. In fact, dropping the test frequency from higher to lower values increased the fatigue crack growth rates specifically in corrosive environments. The case of crack emanating from notches in residual stress fields is shown to be an associated problem affecting the fatigue crack growth rates and the

phenomenon is so complex that it is difficult to cope with the environment sensitive fatigue fracture particularly in the presence of the residual stresses [12–15]. Consequently, it is worth to study the FCG rates in a relaxed residual strain field to understand the applied cyclic stress interaction with regards to frequency and tempering temperature.

In the present work, specimen preparation from a high tensile chain steel, water quenched and tempered, is achieved with the aim to relieve the quenching residual stresses. Subsequently, the fatigue crack growth rates in air are determined using high and low test frequencies in lower and upper bounds of tempering temperatures for the three stages of crack propagation. The results are compared to those reported in the literature using Paris-Erdogan law and an empirical correlation between the exponent n and the constant C is obtained.

2. Experimental approach

2.1. Material and specimen preparation

A high strength alloy steel (DIN 17115) Werkstoff 1.6753 with the specification given in Table I is used in this study. The heat treatment and mechanical properties are shown in Table II, where A and Z are the respective elongation and striction in %.

The material was provided as a round bar. Single edge notched uniaxial specimens were prepared from a 31 mm diameter heat-treated bar as depicted in Fig. 1a. The specimen geometry is based on 'the plane strain fracture toughness of metallic materials', as discussed in ASTM E-399. The heat treatment of 140 mm long bars simulated that used in the manufacturing process of metallic chain element. After one hour quench from 890°C in agitated water, the bar was tempered for three hours at 200°C and 500°C, which were regarded as lower and upper bounds. Then the element was squared to 21 mm × 21 mm and specimens were disk-cut and ground to a final size of 18 × 3.25 mm^2. In this case, to keep a uniform specimen shape, the machining of the gauge length was achieved progressively by removing simultaneous layers of 0.5 mm on each side of the gauge length until about 0.5 mm oversize. At this stage, holes and threads were added and grinding combined with polishing gave the final size of the gauge length. Finally, a starter notch of 2.5 mm was spark-machined using a copper plate electrode to produce a slot of 0.3 mm wide with a root radius of 0.15 mm. The final specimen geometry is given in Fig. 1b.

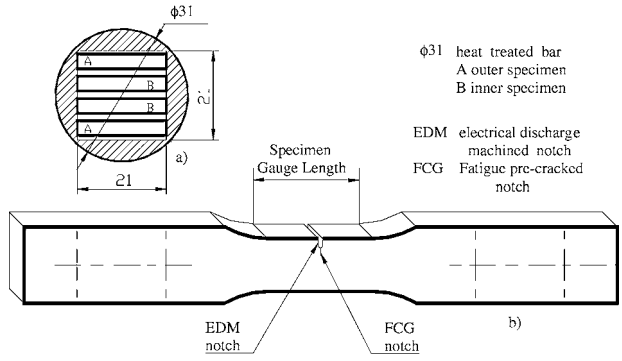

Figure 1 (a) Specimen preparation and (b) Specimen geometry for FCG tests.

2.2. Experimental setup

Fatigue crack growth tests in air were conducted at two frequencies. High frequency fatigue crack growth (FCG) tests were performed at 78 Hz on an Amsler Vibrophore resonant fatigue-testing machine with a mean load of 3 kN and a stress ratio R of 0.1. Whilst FCG at a lower frequency of 0.6 Hz were carried out on a Nene (M3000-S) recirculating ball screw river machine under the same stress ratio conditions. In the beginning, the tests were revealed to be time consuming at the lower frequency since in the same loading conditions no crack growth was observed after 15 days. In order to reduce the initiation time, all specimens were fatigue pre-cracked on the Amsler machine as to get a fine fatigue crack of 1.3 mm.

The surface crack extension was monitored using a travelling optical microscope with a magnitude of 20×. The fatigue crack growth lengths were measured using the direct current potential drop method. It consists of passing a constant current through the specimen and measuring the potential drop between two probes spot-welded to either side of the notch. Hence, the crack length is derived from a predetermined calibration curve. Fig. 2 shows a schematic arrangement and the layout of the equipment. Measured crack lengths are plotted against elapsed number of cycles.

3. Results

3.1. Residual stress

Residual stresses were measured on the specimen blank before notching, using the hole drilling method [24]. In the parent bar after quenching and tempering in the

TABLE I Specifications of W1.6753 for DIN 17115, as supplied

Element	C	Si	S	P	Mn	Ni	Cr	Mo	Al
Specification (Weight%)	0.20	0.25	0.014	0.015	1.48	1.04	0.31	0.46	0.026

TABLE II Mechanical properties of W1.6753 and 35 NCD 16 steels

Material	Quench (°C)	Temp. (°C)	σ_y (MPa)	σ_{max} (MPa)	A (%)	Z (%)	K_{IC} (MNm$^{-3/2}$)
W1.6753	890	200	1293	1477	13.3	64	98
		500	1015	1080	16.5	63	107
35 NCD 16 [20]	875	200	1575	1992	10.7	43.4	71
		500	1295	1512	13.2	51.3	104

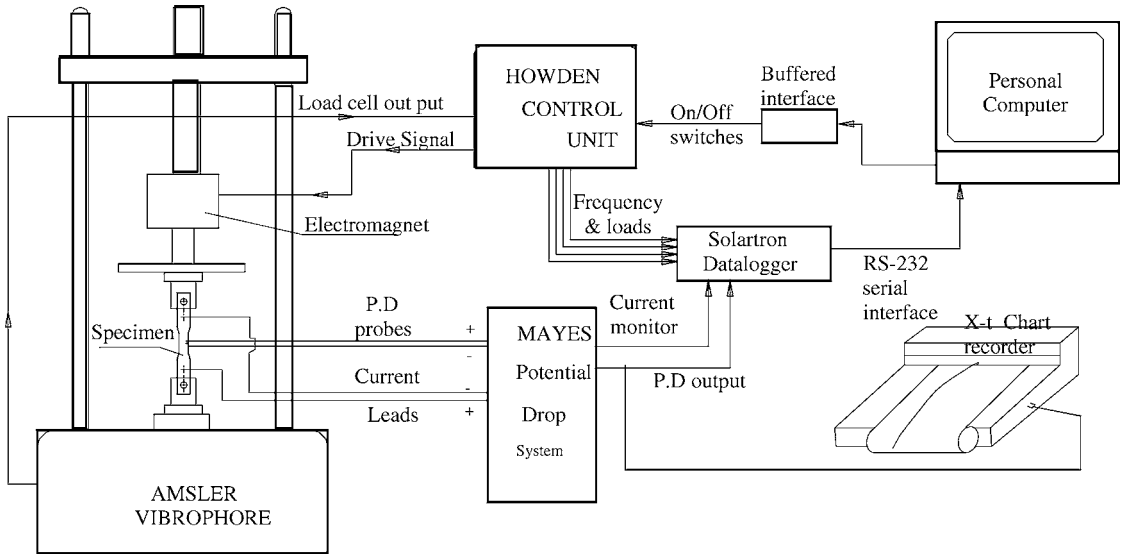

Figure 2 Schematic arrangement and layout of the equipment for FCG tests and crack length measurement.

200°C condition they have been found to be compressive at the surface and tensile within the core [25]. Large-scale values of 230 MPa were obtained in the tensile region whereas compressive stresses at the surface were 340 MPa. As expected, manufacture of thin test pieces relaxed 80% of these stresses. However, tensile stresses continued to act within the core. It should be noted that the machining process of the specimen could have generated the remaining stresses. It is also expected, that as the crack grows, a combination of relief and redistribution of the residual stress will occur as reported in literature [12–14].

3.2. Fractographic observation

Optical fractographic observations were made on a specimen that was fatigue tested at 78 Hz. The test was interrupted for crack length-to-width ratio equal to 0.6; then the specimen was cooled to 77°K in liquid nitrogen and broken to reveal the fracture surface. The morphology of the crack front is depicted in Fig. 3. The EDM notch, followed by the fatigue pre-cracking in zone I where circular beach marks can be observed up to 1.3 mm of a crack depth. Then the fatigue crack propagation in zone II takes places showing ductile fracture [17]. As the crack grows fatigue striations and ligaments get longer to show a stable crack growth associated with thinning of the specimen. Breaking the specimen in liquid nitrogen reveals a clean linear separation between fatigue surface and brittle fracture surface.

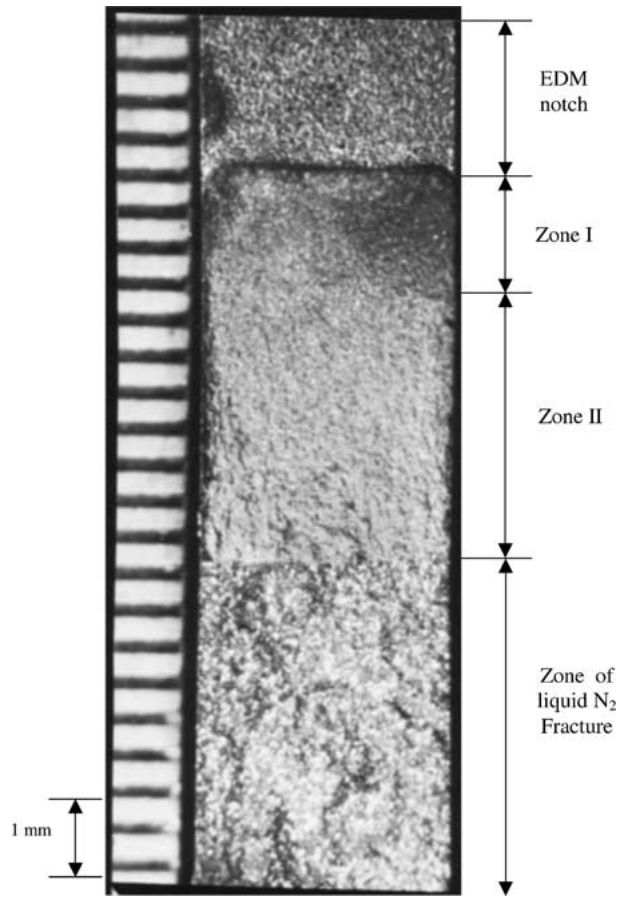

Figure 3 Fracture surface showing crack initiation and propagation in 200°C temp.

3.3. Crack propagation analysis

Crack growth rates were obtained using the secant method suggested by ASTM E647-78T. First, the crack length was measured as a function of elapsed cycles. In practice, it was easy to see from the potential drop when sufficient crack growth had occurred to obtain an accurate measurement. Then the data were subjected to numerical analysis to establish the rate of crack growth. The crack growth rate ($\mathrm{d}a/\mathrm{d}N$) was obtained from the fitted data of the crack length (a) versus number of cycles (N) plot. Values of ($\mathrm{d}a/\mathrm{d}N$) were plotted on log scales as a function of the stress intensity factor range (ΔK_I).

Stress intensity calculations were performed using standard compliance functions following the value of (a/W), as stated by Equations 1 and 2:
For $a/W < 0.6$

$$\Delta K_I = \Delta P/(B \cdot W)(\pi a)^{1/2}[1.12 - 0.23(a/W) + 10.6(a/W)^2 - 21.7(a/W)^3 + 30.4(a/W)^4] \quad (1)$$

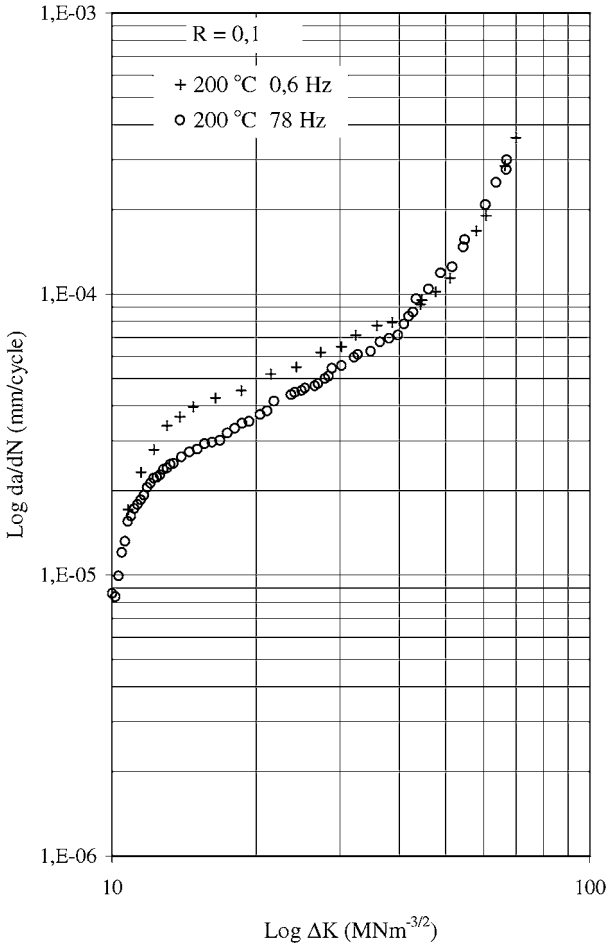

Figure 4 Effect of frequency on fatigue crack growth in air.

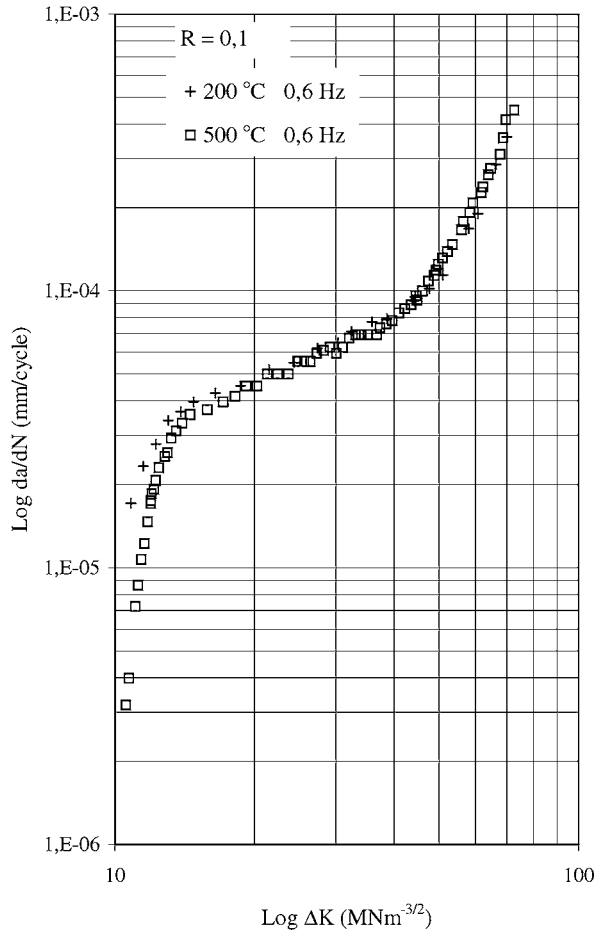

Figure 5 Effect of tempering temperature on fatigue crack growth in air at 0.6 Hz.

For $a/W > 0.6$

$$\Delta K_I = \Delta P/(B \cdot W)(\pi a)^{1/2}[[1.07(1 + 3.03(a/W))] \div [2[\pi a/W(1 - a/W)^{3/2}]^{1/2}]] \quad (2)$$

where ΔP and B are the mean applied load and the specimen thickness respectively.

The obtained plots are presented in Figs 4–6. A typical sigmoidal curve is observed showing a near threshold region where the crack grows faster, then a linear region where Paris-Erdogan law [26] can be applied, followed by an unstable region as specimen failure occurs. In order to complete the analysis, the Paris-Erdogan law [26]:

$$da/dN = C(\Delta K_I)^n \quad (3)$$

is used to establish the profile of the stable FCG region as a function of frequency and tempering temperature.

4. Discussion

The effect of frequency is illustrated in Fig. 4 as a plot of the da/dN versus ΔK_I for the 200°C temper condition. It is observed that at above 10^{-5} mm/cycle, FCG rates for tests conducted at 0.6 Hz were up to 1.5 higher than those conducted at 78 Hz, in the near threshold region. Generally, the reported data are plotted without any reference to frequency effect from 0.1 to 100 Hz and it is shown that even the change of the cyclic wave form does not affect the rates of FCG over this frequency range [21–23].

In the present case, the observed difference in FCG rates may be associated with the presence of air at the crack tip [3, 21, 22]. A similar behavior has been obtained in the case of two high strength aluminum alloys, where in stage II, low frequency shows higher FCG rate [27]. In fact, in the early stage crack growth, oxidation at the crack tip finds some time to take place and allows air oxidation to enhance the mechanical FCG rate. As the crack gets longer, the oxide film has not enough time to occur and looses its effects, therefore the linear slopes of the FCG curves meet together when approaching the unstable region.

The effect of tempering temperature on fatigue crack growth constitutes a continual subject of interest for many workers [28–30]. Figs 5 and 6 show the effect of tempering temperature at 78 and 0.6 Hz. In the first case, the behavior of FCG rates for the 200°C temper condition (Fig. 5), is almost identical except for ΔK_I between 10 to 17 $MNm^{3/2}$. Here, ΔK_I approaches the near threshold region therefore ΔK_{th} must be considered. The behavior of FCG rates is sensitive to many parameters [3, 4, 17, 18] and follows that of the threshold region. It is worth noting that for 200°C temper, with higher yield stress, the size of the plastic zone ahead of the crack is smaller, leading to the acceleration of FCG rates. However, in terms of residual stresses, the effect is related to changes in R ratio with regards to global stress distribution, resulting in different values

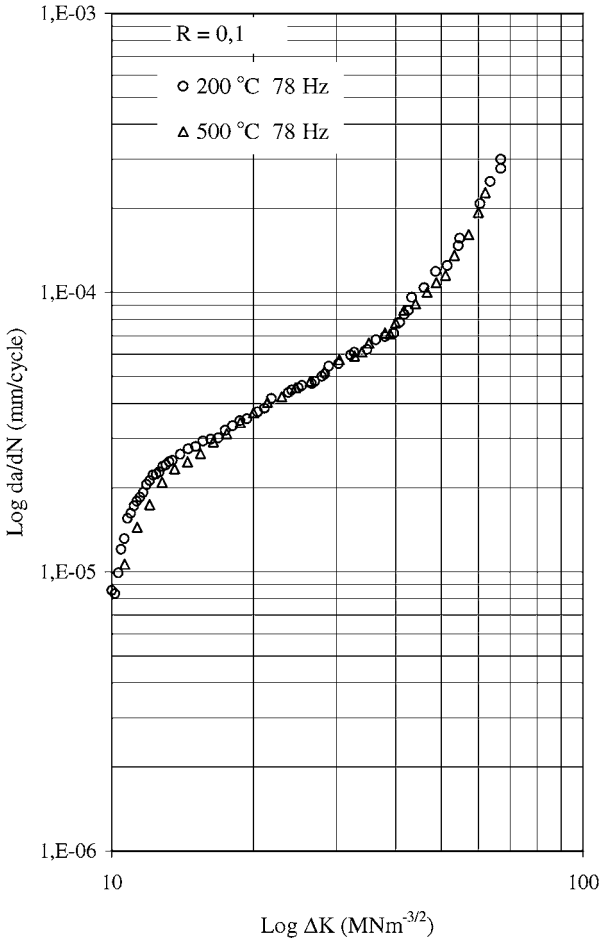

Figure 6 Effect of tempering temperature on fatigue crack growth in air at 78 Hz.

of R and ΔK_I as suggested by literature [12, 13, 32]. In the second case, at 0.6 Hz, for the 500°C temper condition it was possible to measure very low rates in the order of 3.2×10^{-6} mm/cycle and the gap between both temper conditions is almost one order magnitude for ΔK_I close to 10 $MNm^{-3/2}$ (Fig. 6). Mainly, significant differences are observed in FCG in the near threshold region. The lower the temper condition, the higher the crack growth rate at both frequencies. On the other side, the lower the frequency, the higher the FCG for both temper conditions. As far as W1.6753 steel investigation is concerned, a previous study [16] revealed that in the threshold region, FCG rates are faster for low tempering temperatures, which is confirmed by this study. Above 17 $MNm^{-3/2}$ the effect of tempering temperature becomes nil and no significant effect of frequency or tempering is distinguishable.

In order to complete the FCG in stage II, the parameters describing Paris—Erdogan law [26] are obtained using a computer linear correlation for the prescribed data. The results are summarized in Table III. Basically, it is observed that higher frequencies show higher n and lower values of C for either tempering temperatures. In the case of W1.6753 steel, when comparing with high strength steel, identified as 35 NCD 16 steel [20], it is concluded that at 25 Hz all the n values were two folds higher whereas the C values were almost two order magnitude lower (Table III). Although the mechanical properties of 35 NCD 16 steel are better, the measured fracture toughness (K_{IC}) of W1.6753 remains the controlling parameters of FCG as indicated in Table II.

TABLE III Comparison between the material constants n and Log C

Material	Temp. (°C)	Frequency	n	Log C
W1.6753	200	0.6	1.06	4.60E-06
	200	78	1.2	2.00E-06
	500	0.6	1.07	3.50E-06
	500	78	1.21	1.50E-06
35NCD16 [20]	200	25	2.69	1.94E-08
	300		2.36	5.53E-08
	400		2.54	3.12E-08
	500		2.05	1.48E-07

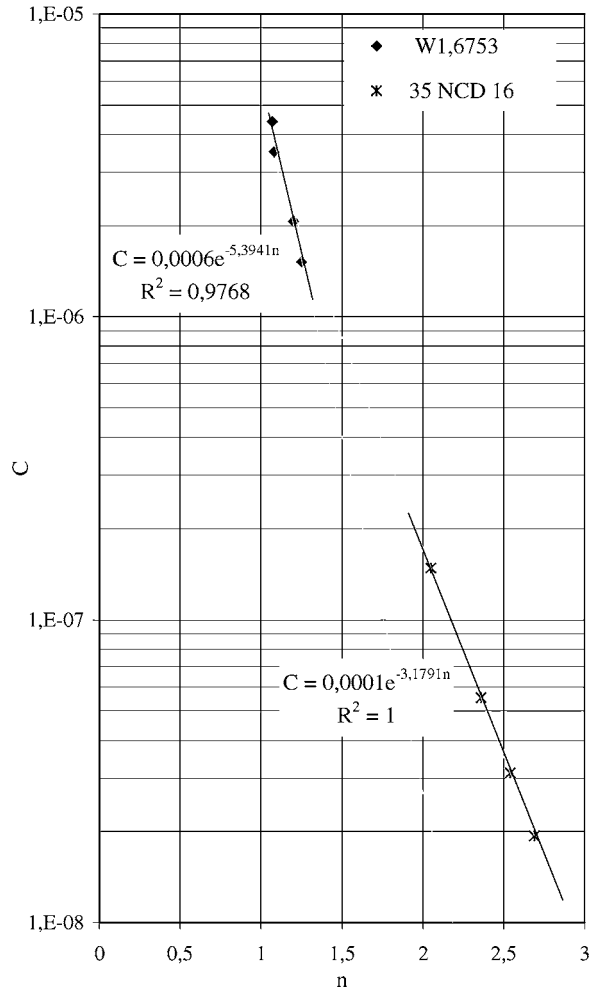

Figure 7 Relationship between n and C for two chain steels tested in air W1.6753 steel at 0.6 and 78 Hz; 35 NCD 16 steel [20] at 25 Hz.

At this stage, it is interesting to study the correlation between C and n as a function of testing frequency and tempering temperature. To achieve this goal, a plot of Log C as a function of n is constructed (Fig. 7). The analysis shows a linear relationship between the two parameters of the Paris-Erdogan equation suggesting a mutual dependence between C and n in the form of:

$$n = a \operatorname{Log} C + b \tag{4}$$

This type of equation has already been presented by others [3, 32–35] and the significant result is the vanishing of the effect of frequency and temper conditions

for this material. It has been proven earlier that the same approach permitted to study the effect of applied stress in the case of commercial steel [36] and to conclude with one equation in the form of Equation 3 describing stage II of FCG. Using Equations 3 and 4, the rate of fatigue crack growth for W1.6753 steel can be written as:

$$da/dN = 6 \cdot 10^{-4} e^{-5.3941n} (\Delta K_I)^n \qquad (5)$$

Similarly, for 35 NCD 16 steel, the FCG equation controlling stage II may be put as:

$$da/dN = 10^{-4} e^{-3.1751n} (\Delta K_I)^n \qquad (6)$$

with da/dN in mm/cycle and ΔK_I in $MNm^{-3/2}$. The determination coefficient (r^2) for both Equations 5 and 6 are 1.0 and 0.98 respectively. Equation 5 includes at the same time the effect of both frequency and tempering conditions. The results are basically in good agreement with those found in the literature [33–36]. A survey of reported results on the relationship between n and C indicates that the curves are equidistant and the coefficient b (Equation 4) is function of Young's modulus [37].

5. Conclusion

Fatigue crack growth tests have been carried out in air environment on typical high tensile mining chain steel at different conditions of cycling and tempering. It is found for W1.6753 steel that in the near threshold region, lowering the tempering temperature resulted in an increase of the FCG at 0.6 Hz and 78 Hz. In addition, FCG increased when frequency is changed from 78 Hz to 0.6 Hz for both 500°C and 200°C tempering temperatures. The effects of frequency and tempering temperature are well described by the Paris-Erdogan law expressed as a power relationship of the form:

$$da/dN = Ae^{\beta n} (\Delta K_I)^n \qquad (7)$$

where $A = 6 \cdot 10^{-4}$ and $\beta = -5.3941$ for W1.6753 steel. Furthermore, for this high tensile chain steel, the FCG prediction is expressed as a function of a single variable n.

Acknowledgements

The experimental work has been conducted at the Material Research Laboratory of the Mechanical Department at the Faculty of Engineering of Bristol University in the UK, with the grateful help of Professor W. J. Plumbridge.

References

1. A. CARPINTIERI (ed.), "Handbook of Fatigue Crack Propagation in Metallic Structures" (Elsevier, Amsterdam, 1994).
2. G. LUTJERING and H. NOWACK, "Fatigue '96" (Pergamon, Oxford, 1996).
3. C. BATHIAS and J. P. BAÏLON, "La fatigue des matériaux et des structures," 2nd ed. (HERMES, Paris, 1997).
4. S. SURESCH, "Fatigue of Materials," 2nd ed. (Cambridge University Press, Cambridge, 1998).
5. T. W. TSAY, C. S. CHUNG and C. CHEN, *Int. J. Fatigue* **19** (1997) 25.
6. T. OCHI, H. KANISAWA, K. OOKI and Y. KUSANO, *Nippon Steel Technical Report* **80** (1999) 19.
7. H. DI FANT-JAECKELS and A. GALTIER, *La Revue de Metallurgie-CIT* **1** (2000) 83.
8. X. KEWEI and H. JIAWEN, *Eng. Fracture Mech* **41**(3) (1992) 405.
9. B. D. HORN, *Iron and Steel Engineer* **73** (1996) 49.
10. A. C. BATTISTA, A. M. DIAS, P. VIRMINEUX, G. INGLEBERT, T. HASSINE, J. C. LE FLOUR and J. L. LEBRUN, in 10th Int. Conf, Lisbon, Portugal (1994) p. 739.
11. S. R. DANIEWICZ, J. A. COLLINS and D. R. HOUSER, *Int. J. Fatigue* **16**(2) (1994) 123.
12. J. H. UNDERWOOD, L. P. POOK and J. K. SHARPLES, *ASTM STP* **631** (1977) 402.
13. G. GLINKA, *ibid.* **677** (1979) 198.
14. R. J. BUCCI, in *Fracture mechanics*: 13th Conference. *ibid.* **743** (1981) 28.
15. A. P. PARKER, *ibid.* **776** (1981) 13.
16. W. J. PLUMBRIGE and N. KNEE, *Scri. Metall.* **19** (1985) 1029.
17. J. E. KING and W. GEARY, *IMechE*, **C243/86** (1986) 417.
18. W. ELBER, *ASTM STP* **486** (1971) 230.
19. H. MAYER, *International materials reviews* **44**(1) (1999) 1.
20. A. O. BAUS, J. C. CHARBONNIER, H. P. LIEURADE, B. MARANDET, I. ROESH and G. SANZ, *IRSID Report* **P 240** (1975) 1703.
21. R. P. WEI, *ASTM STP* **675** (1979) 816.
22. J. M. BARSOM, in "Corrosion Fatigue: Chemistry, Mechanics and Microstructure" (National Association of Corrosion Engineers, NACE-**2**, 1972) p. 424.
23. A. BIGNONNET, *La Revue de Metallurgie-MES*, **1** (1989) 17.
24. E. M. PROCTER and E. PROCTER, *Strain* **10**(1) (1974) 7.
25. A. AMIRAT and W. J. PLUMBRIDGE, in Proceeding of 10th International Conference on Experimental Mechanics, Lisbon (1994) 805.
26. P. PARIS and F. ERDOGAN, *J. Basic Eng., Transaction ASME* **85** (1963) 528.
27. J. C. RADON, *Corrosion Fatigue, Metal Science* **13** (1979) 411.
28. G. MARQUIS and J. SOLIN, "Fatigue Design and Reliability" (Elsevier, Amsterdam, 1999).
29. D. MIANNAY, P. COSTA, D. FRANCOIS, A. PINEAU and M. BERVEILLER, "Advances in Mechanical Behaviour, Plasticity and Damage" (Elsevier, Amsterdam, 2000).
30. X. Q. SHIM, H. L. J. PANG, W. ZHOU and Z. P. WANG, *Int. J. fatigue* **22** (2000) 217.
31. R. GALATOLO and A. LANCIOTTI, *Int. J. fatigue* **19** (1997) 43.
32. D. V. NELSON, *Experimental Mechanics* **17** (1977) 41.
33. L. N. McCARTNEY and P. E. IRWING, *Science of Metallurgy* **11** (1977) 181.
34. J. P. BENSON and D. V. EDMONDS, *ibid.* **12** (1978) 645.
35. E. H. NICCOLLS, *Science of Metallurgy* **10** (1976) 295.
36. G. Ö. BILIR and F. HAZNEDAR, *Int. J. Fracture* **37** (1988) 73.
37. J. MASSOUNAVE, J. P. BAILON and J. L. DICKSON, in "La fatigue des matériaux et des structures," 2nd ed., Paris, HERMES (1997) ch. 6, p. 255.

Received 25 October 2001
and accepted 9 September 2002